The Intensity of Singularity of Residual Thermal Stresses at A Vertex in Three-Dimensional Bonded Structures

H. Koguchi[1], T. Taniguchi[2]
[1]*Nagaoka University of Technology, Nagaoka, Japan;* [2]*Shin-Etsu Chemical Co., Ltd, Takasaki, Japan*

1. Introduction

The authors have been investigated the characteristic of stress singularity fields at a vertex on an interface in two- and three-dimensional bonded joints [1,2,3]. It is well known that stress distribution in stress singularity fields can be expressed as a function of distance from a stress singular point. In two-dimensional joints, an angular variation for the stress distribution in a polar coordinate system with an origin at the stress singular point can be expressed analytically based on the theory of elasticity [4,5,6,7]. On the contrary, in three-dimensional joints[8], an angular variation of stress distribution in a spherical coordinate system cannot be clearly expressed until now. For instance, stress singularity line which is a cross line with an interface and a side free surface will affect on the stress distribution near the vertex. Generally, stress distribution in the stress singularity region can be expressed as follows.

$$\sigma_{ij}(r,\theta,\phi) = \sum_m K_m r^{-\lambda_m} f_{ij}^m(\theta,\phi) \tag{1}$$

Here, r represents the distance from the stress singular point, K_m the intensity of singularity, $f_{ij}^m(\theta,\phi)$ the angular function for stress distribution, and λ_m the order of stress singularity. In the present paper, a material combination in electronic

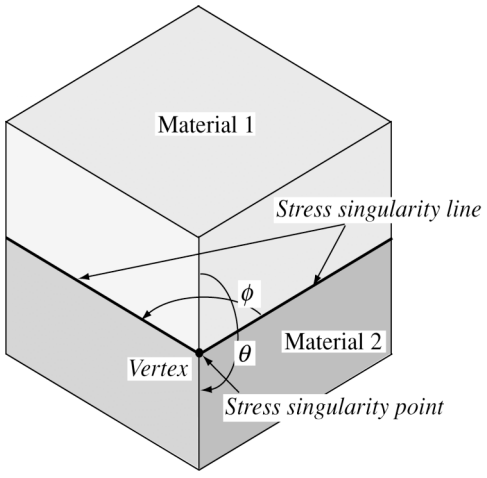

Fig.1 Three-dimensional bonded structures

devices is used and the distribution of residual thermal stress near the vertex in three-dimensional joint structures is precisely investigated. In particular, the order of singularity is determined using an eigen equation based on a finite element formulation, and angular functions, $f_{ij}(\theta,\phi)$, for stress distribution determined from eigen vector will be compared with the distribution of residual thermal stress calculated using BEM. The intensity of singularity at the vertex in three-dimensional joints will be determined considering stress singularity lines.

2. Analysis

2.1 Method for analysis

In the present paper, residual thermal stresses are calculated using BEM. The expression for boundary integral equation is shown below.

$$c_{ij}(P)u_j(P) = \int_\Omega U_{ij}^*(P,Q)t_j dS(Q) - \int_\Omega T_{ij}^*(P,Q)u_j dS(Q) \qquad (2)$$

where c_{ij} represents constant depending on the geometry of boundary, Ω the boundary in the domain for analysis, U_{ij}^* and T_{ij}^* are fundamental solutions for displacement and traction, respectively. P and Q are observation and source points on the boundary. t_i and u_i are traction and displacement vectors, respectively. In the present paper, Rongved's solution for two-phase isotropic materials is used for analysis as the fundamental solutions. Hence, mesh division on an interface in joints is not required for analysis.

Eigen equation using a finite element method was formulated for determining the order of stress singularity as follows[9].

$$\left(p^2[A] + p[B] + [C]\right)\{u\} = 0 \qquad (3)$$

where p represents the characteristic root, which is related to the order of singularity, λ, as λ=1-p. [A], [B] and [C] are matrices composed of material properties, and {u} represents the displacement vector.

In the present paper, thermal residual stress is determined following Duhamel's theorem. When isotropic and homogeneous materials are subjected to a temperature variation of ΔT, thermal strain ε_{ij}^T can be expressed as

$$\varepsilon_{ij}^T = \alpha \cdot \Delta T \, . \qquad (4)$$

where α represents the coefficient of thermal expansion, and δ_{ij} Kronecker's delta. When thermal expansion is constrained, thermal stress occurs. Material follows Hooke's law, and then a relationship between stress and strain is expressed as follows.

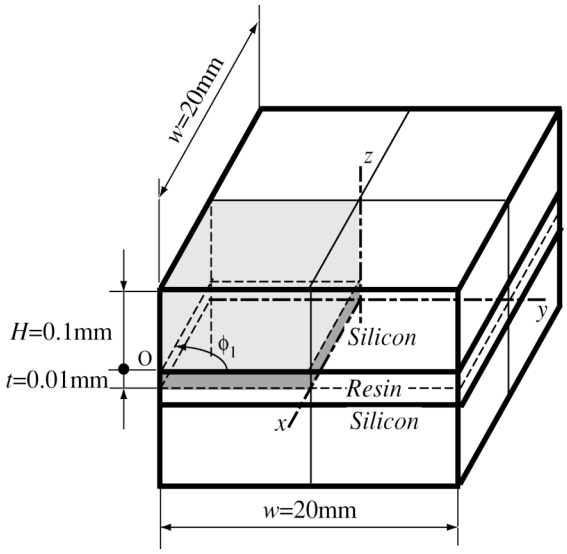

Fig.2 Bonded structure for analysis

$$\sigma_{ij} = \frac{E}{1+\nu}\left(\varepsilon_{ij} + \frac{\nu}{1-2\nu}\varepsilon_{kk}\delta_{ij}\right) - \frac{E}{1-2\nu}\alpha\Delta T\delta_{ij} \tag{5}$$

where E represents Young's modulus, and ν Poisson's ratio. In calculating the residual thermal stress, stress analysis for the joint on side surfaces subjecting to $E\alpha\Delta T/(1-2\nu)$ is firstly carried out, and the applied stress is secondly subtracted from the results of stress distribution.

Model for analysis is shown in Fig.2. The size of silicon is 0.1mm in height and 20mm in width. The thickness of interlayer (resin) is 0.01mm. Material properties used in the analysis are shown in Table 1.

Table 1 Material properties used in analysis

	Young's modulus	Thermal expansion	Poisson's ratio	Thermal stress
	E [GPa]	A [$\times 10^{-6}$ K^{-1}]	ν	σ_{th} [MPa]
Silicon	166	0.30	0.26	161
Resin	2.74	33	0.38	58.4

3. Results and Discussion

3.1 Eigen analysis

Mesh division for eigen analysis is shown in Fig.3. Figure 3(*a*) represents mesh on a unit sphere with an origin at the vertex. Figure 3(*b*) shows the developed $\theta\times\phi$ plane of the sphere surface. In the present paper, two eigen analyses were

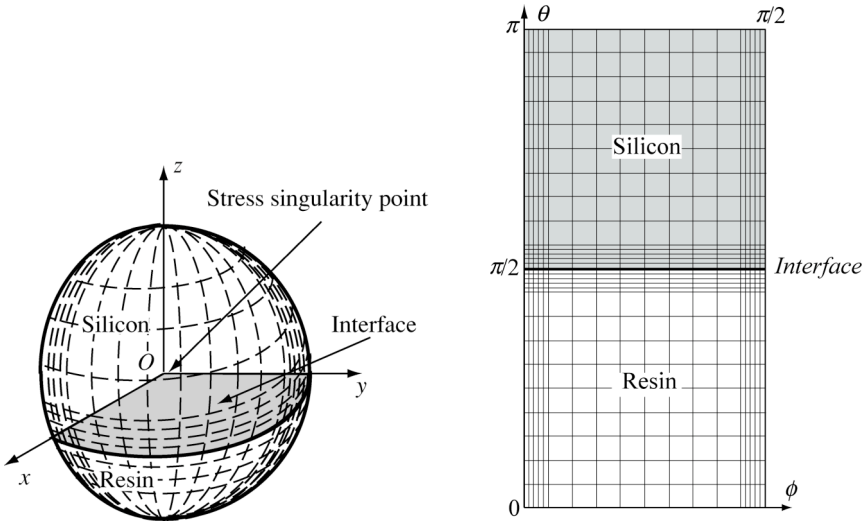

(*a*) A mesh divison of the surface of a unit sphere with the origin at the vertex

(*b*) A mesh on the developed $\theta\times\phi$ plane

Fig.3 FEM model for eigen analysis

Table 2 The order of stress singularity

The order of singularity		
	$\phi_1=\pi/2$	$\phi_1=\pi$
	p_{vertex} λ_{vertex}	p_{side} λ_{side}
1	1.000 0.000	1.000 0.000
2	1.000 0.000	1.000 0.000
3	1.000 0.000	1.000 0.000
4	0.606 0.395	1.000 0.000
5	- -	1.000 0.000
6	- -	0.682 0.318

conducted to obtain the order of stress singularity at the vertex and at a point on a stress singularity line. The results of eigen analysis are shown in Table 2. Symbol ϕ_1 in Table 1 indicates an angle between two stress singularity lines on the interface shown in Fig.2. It is found that a triple root of p=1 in $\phi_1=\pi/2$ and a quintuple root of p=1 in $\phi_1=\pi$ exist. From the previous paper[10], it is shown that a repeated root exists, and then the logarithmic singularity occurs. Stress in the stress singularity field can be expressed as

$$\sigma_{ij}^{s}(\bar{r},\theta,\phi)=K_{1ij}^{s}f_{1ij}(\theta,\phi)\bar{r}^{-\lambda}+K_{2ij}^{s}f_{2ij}(\theta,\phi)+\sum_{k=3}^{M}K_{kij}^{s}f_{kij}(\theta,\phi)(\ln\bar{r})^{k-2} \qquad (6)$$

where $\bar{r}=r/t$, M=4 ($\phi_1=\pi/2$) and 6 ($\phi_1=\pi$), and K_{kij}^{s} represents the intensity of singularity.

Angular functions for stress components obtained from eigen analysis in Eq.(3) are examined. In the present paper, angular functions of $f_{\theta\theta}$, $f_{r\theta}$ and $f_{\theta\phi}$ corresponding to the modes I, II and III at the crack tip are precisely investigated. Figure 4 represents the distribution of angular function, f_{ij}, on the θ-ϕ plane. In these figures, the value of f_{ij} is normalized using the value of $f_{\theta\theta}$ at $\phi=\pi/4$ and $\theta=\pi/2$. The angular functions cannot be normalized by the maximum values, because $f_{\theta\theta}$ and $f_{\theta\phi}$ have a singularity at $\theta=\pi/2$ and $\phi=0$, $\pi/2$, where stress singularity lines exist.

Angular functions, f_{ij}, distributed on the unit sphere shown in Fig.2 may be characterized by a distance from a stress singularity line. Stress distribution in a cross section, APQ, shown in Fig.5 can be expressed using a power law with the order of singularity for the stress singularity line with an origin at the point A. ρ_{AP} represents the distance from a point A on the stress singularity line to a point P on the unit sphere. Here, the angular functions on the stress singularity line can be expressed as follows.

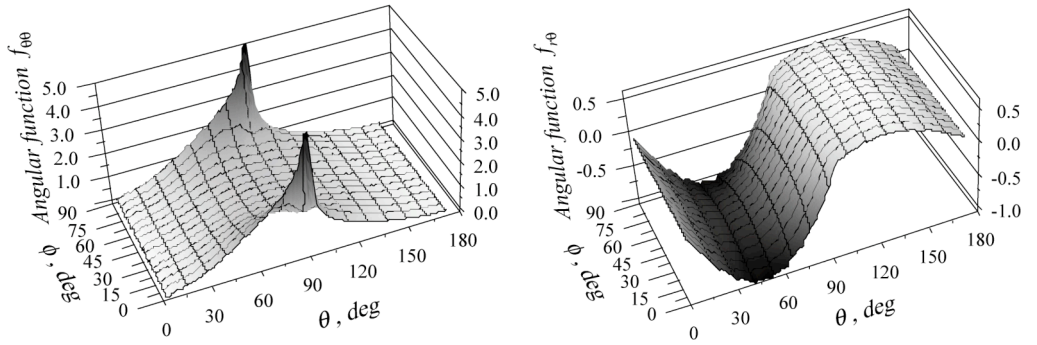

(a) Distribution of angular function $f^s_{\theta\theta}$ (b) Distribution of angular function $f^s_{r\theta}$

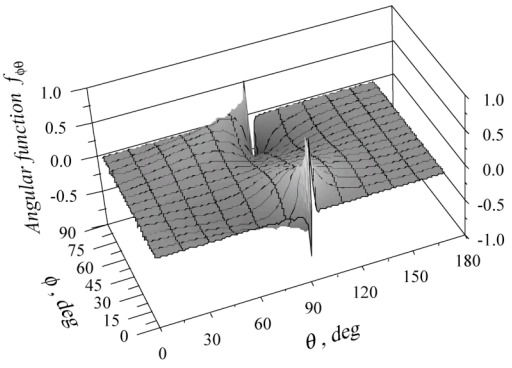

(c) Distribution of angular function $f^s_{\phi\theta}$

Fig. 4 Distributions of angular function f^s_{ij} on the θ–ϕ plane

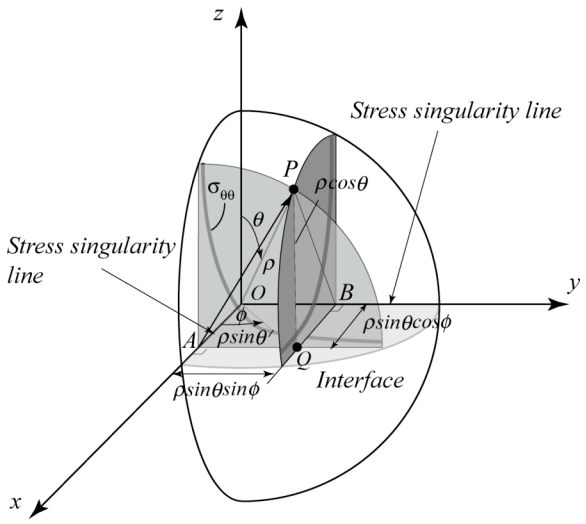

Fig.5 Stress singularity line near the vertex

$$h_{ij}^{l}\left(\rho_{AP},\Theta\right)=L_{1ij}^{l}\rho_{AP}^{-\lambda_{side}}g_{1ij}^{l}\left(\Theta\right)+L_{2ij}^{l}g_{2ij}^{l}\left(\Theta\right)+\sum_{k=3}^{6}L_{kij}^{l}g_{kij}^{l}\left(\Theta\right)\left(\ln\rho_{AP}\right)^{k-2} \qquad (7)$$

where Θ represents the angle between AP and AQ, $\rho_{AP}=\rho\sqrt{1-\sin^2\theta\cos^2\phi}$. Angular functions in spherical coordinate system with the origin at the vertex can be obtained by transforming from cylindrical coordinate system. Angular functions, $f_{\theta\theta}^{s}$, $f_{r\theta}^{s}$, $f_{\phi\theta}^{s}$, on the interface (at Θ=0) is expressed using the angular function for stress components in the cylindrical coordinate system as follows.

$$\begin{aligned}
f_{\theta\theta}^{s}&=h_{\Theta\Theta}^{l}\\
f_{r\theta}^{s}&=-h_{R\Theta}^{l}\sin\phi-h_{x\Theta}^{l}\cos\phi\\
f_{\phi\theta}^{s}&=-h_{R\Theta}^{l}\cos\phi+h_{x\Theta}^{l}\sin\phi
\end{aligned} \qquad (8)$$

Here, $h_{x\Theta}^{l}$ represents the angular function for $\sigma_{x\Theta}$. Substituting Eq.(7) into Eq.(8) yields

$$f_{\theta\theta}^{sA}\left(\phi\right)=L_{1\Theta\Theta}^{A}\left(\sin\phi\right)^{-\lambda_{side}^{A}}g_{1\Theta\Theta}^{Al}\left(0\right)+L_{2\Theta\Theta}^{A}g_{2\Theta\Theta}^{Al}\left(0\right)+\sum_{k=3}^{6}L_{k\Theta\Theta}^{A}g_{k\Theta\Theta}^{Al}\left(0\right)\left\{\ln\left(\sin\phi\right)\right\}^{k-2}$$

$$f_{r\theta}^{sA}\left(\phi\right)=-L_{1R\Theta}^{A}\left(\sin\phi\right)^{1-\lambda_{side}^{A}}g_{1R\Theta}^{Al}\left(0\right)-L_{2R\Theta}^{A}g_{2R\Theta}^{Al}\left(0\right)\sin\phi$$

$$-\sum_{k=3}^{6}L_{kR\Theta}^{A}g_{kR\Theta}^{Al}\left(0\right)\sin\phi\left\{\ln\left(\sin\phi\right)\right\}^{k-2}-L_{1x\Theta}^{A}\left(\sin\phi\right)^{-\lambda_{side}^{A}}\cos\phi\;g_{1x\Theta}^{Al}\left(0\right)$$

$$-L^{A}_{2x\Theta}g^{Al}_{2x\Theta}(0)\cos\phi-\sum_{k=3}^{6}L^{A}_{kx\Theta}g^{Al}_{kx\Theta}(0)\cos\phi\left\{\ln(\sin\phi)\right\}^{k-2}$$

$$f^{sA}_{\phi\theta}(\phi)=-L^{A}_{1R\Theta}(\sin\phi)^{-\lambda^{A}_{side}}\cos\phi g^{Al}_{1R\Theta}(0)-L^{A}_{2R\Theta}g^{Al}_{2R\Theta}(0)\cos\phi$$
$$-\sum_{k=3}^{6}L^{A}_{kR\Theta}g^{Al}_{kR\Theta}(0)\left\{\ln(\sin\phi)\right\}^{k-2}\cos\phi+L^{A}_{1x\Theta}(\sin\phi)^{1-\lambda^{A}_{side}}\,g^{Al}_{1x\Theta}(0)$$
$$+L^{A}_{2x\Theta}g^{Al}_{2x\Theta}(0)\sin\phi+\sum_{k=3}^{6}L^{A}_{kx\Theta}g^{Al}_{kx\Theta}(0)\sin\phi\left\{\ln(\sin\phi)\right\}^{k-2} \qquad (9)$$

Here, the superscript A in f^{sA}_{ij} indicates that the angular functions correspond to the stress singularity line OA. It is found from Eq.(9) that $f^{sA}_{\theta\theta}$, $f^{sA}_{\phi\theta}$ and $f^{sA}_{r\theta}$ have a singularity for the singularity line as ϕ approaches to zero. Figure 6 represents the distributions of angular function, $f_{\theta\theta}$, $f_{r\theta}$ and $f_{\phi\theta}$ on the interface. Considering the influence of the stress singularity line, OB, on the stress distribution near the vertex and the symmetry of angular functions with respect to $\phi=\pi/4$, angular functions in the spherical coordinate can be expressed as

$$f^{s}_{\theta\theta}=f^{sA}_{\theta\theta}(\phi)+f^{sB}_{\theta\theta}\left(\frac{\pi}{2}-\phi\right)$$
$$f^{s}_{r\theta}=f^{sA}_{r\theta}(\phi)+f^{sB}_{r\theta}\left(\frac{\pi}{2}-\phi\right) \qquad (10)$$
$$f^{s}_{\phi\theta}=f^{sA}_{\phi\theta}(\phi)-f^{sB}_{\phi\theta}\left(\frac{\pi}{2}-\phi\right)$$

For simplicity, some coefficients are arranged like as $L^{M*}_{k\theta\theta}=L^{M}_{k\Theta\Theta}g^{Ml}_{k\Theta\Theta}(0)$, ($M$=$A$,

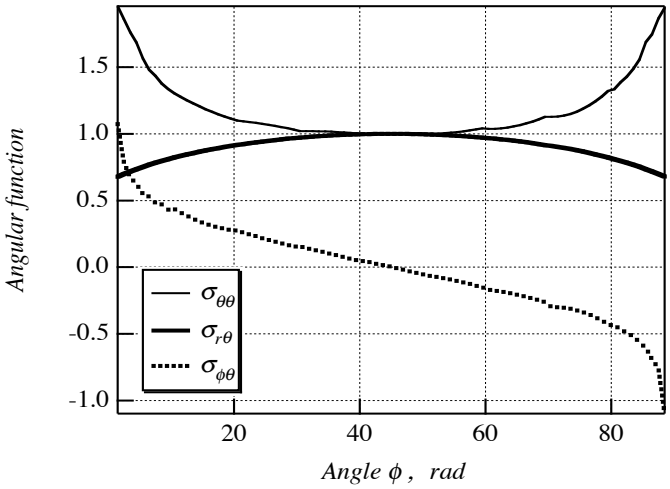

Fig.6 Angular functions at the interface $\theta=\pi/2$

B), etc. and these coefficients are set to be $L_{kij}^{A*} = L_{kij}^{B*} = L_{kij}^{*}$ in the present model. Furthermore, logarithmic terms in the expressions are neglected, and then coefficients in the angular functions are determined using a least square method for plots shown in Fig.6.

Table 3 Coefficients of angular functions

	$f_{\theta\theta}^{s}$		$f_{r\theta}^{s}$		$f_{\phi\theta}^{s}$	
Power law term	$L_{1\theta\theta}^{*}$	0.6493	$L_{1r\theta}^{*}$	-0.0037	$L_{1\phi\theta}^{*}$	0.2891
2nd term	$L_{2\theta\theta}^{*}$	-0.4566	$L_{2r\theta}^{*}$	0.7165	$L_{2\phi\theta}^{*}$	-0.0171
3rd term	-	-	$L_{3r\theta}^{*}$	-0.0088	-	-

Substituting the angular functions, f_{ij}^{s}, into Eq.(6) yields

$$
\begin{aligned}
&\sigma_{\theta\theta}^{s}(r,\pi/2,\phi) = K_{1\theta\theta}^{s}\left[L_{1\theta\theta}^{*}\left\{(\sin\phi)^{-\lambda_{side}} + (\cos\phi)^{-\lambda_{side}}\right\} + L_{2\theta\theta}^{*}\right]\bar{r}^{-\lambda_{ver}} \\
&+K_{2\theta\theta}^{s} f_{2\theta\theta}(\pi/2,\phi) + \\
&\sigma_{r\theta}^{s}(\bar{r},\pi/2,\phi) = K_{1r\theta}^{s}\left[L_{1r\theta}^{*}\left\{(\sin\phi)^{-\lambda_{side}}\cos\phi + (\cos\phi)^{-\lambda_{side}}\sin\phi\right\}\right. \\
&\left.+L_{2r\theta}^{*}\left\{(\sin\phi)^{1-\lambda_{side}} + (\cos\phi)^{1-\lambda_{side}}\right\} + L_{3r\theta}^{*}(\sin\phi+\cos\phi)\right]\bar{r}^{-\lambda_{ver}} \qquad (11) \\
&+K_{2r\theta}^{s} f_{2r\theta}(\pi/2,\phi) + \\
&\sigma_{\phi\theta}^{s}(\bar{r},\pi/2,\phi) = K_{1\phi\theta}^{s}\left[L_{1\phi\theta}^{*}\left\{(\sin\phi)^{-\lambda_{sideA}}\cos\phi - (\cos\phi)^{-\lambda_{sideB}}\sin\phi\right\}\right. \\
&\left.+L_{2\phi\theta}^{*}(\cos\phi-\sin\phi)\right]\bar{r}^{-\lambda_{ver}} + K_{2\phi\theta}^{s} f_{2\phi\theta}(\pi/2,\phi) +
\end{aligned}
$$

3.2 BEM analysis

Distributions of residual thermal stresses are obtained using BEM and are shown in Fig.7. These figures represent the distributions on the interface against the distance from the vertex. Plots for various angles ϕ is parallel to each other and a plot for $\phi=\pi/4$ shows the smallest value at the same $\bar{r}$ (=r/t) in $\sigma_{\theta\theta}$ and $\sigma_{\phi\theta}$ except $\sigma_{r\theta}$. Figure 8 shows the distribution of $\sigma_{\theta\theta}$, $\sigma_{r\theta}$ and $\sigma_{\phi\theta}$ against ϕ at $\bar{r}$ =0.01. Stress distribution shown in Fig.8 is similar to the distribution of angular functions, f_{ij}, against ϕ. In this figure, all stresses are normalized by the value of $\sigma_{\theta\theta}$ at $\phi=\pi/4$ and $\theta=\pi/2$.

Coefficients, K_{1ij}, of Eq.(11) for the plots of $\sigma_{\theta\theta}$ and $\sigma_{r\theta}$ at $\phi=\pi/4$ and $\sigma_{\phi\theta}$ at $\phi=\pi/6$ in Fig.7 are determined using a least square method. The coefficients of Eq.(11) are listed in Table 4.

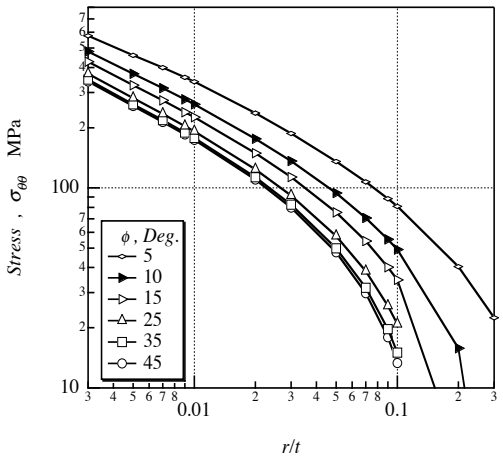

(a) Stress $\sigma_{\theta\theta}$

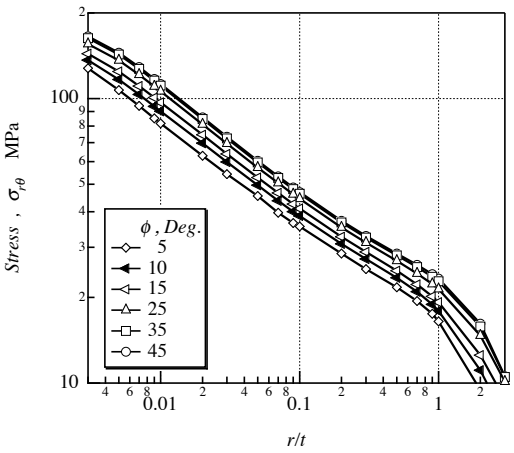

(b) Stress $\sigma_{r\theta}$

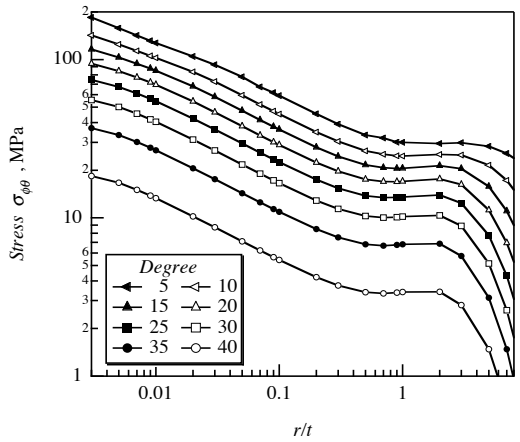

(c) Stress $\sigma_{\phi\theta}$

Fig. 7 Distributions of stress for r/t

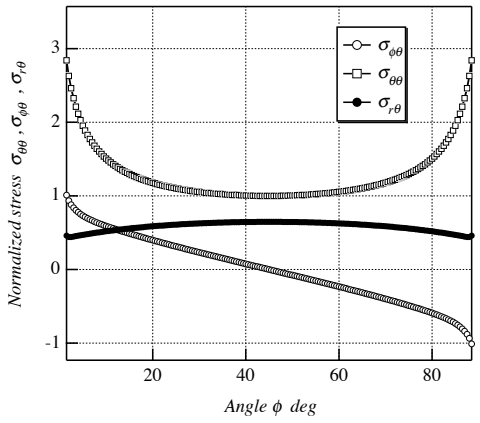

Fig.8 Distributions of stress against ϕ

Table 4 Coefficients of Eq.(11)

$K^s_{1\theta\theta}$	43.74	$K^s_{1r\theta}$	17.68	$K^s_{1\phi\theta}$ (at ϕ=30deg)	41.09
$K^s_{2\theta\theta}$	-95.62	$K^s_{2r\theta}$	2.93	$K^s_{2\phi\theta}$ (at ϕ=30deg)	1.01

Table 5 The intensity of singularity

$K^{3D}_{\theta\theta}$, MPa	28.4	$K^{3D}_{r\theta}$, MPa	-0.065	$K^{3D}_{\theta\phi}$, MPa	11.88

Equation (11) can be arranged as

$$\sigma^s_{\theta\theta}(r,\pi/2,\phi) = K^s_{1\theta\theta}L^*_{1\theta\theta}\left[(\sin\phi)^{-\lambda_{side}} + (\cos\phi)^{-\lambda_{side}} + L^*_{2\theta\theta}/L^*_{1\theta\theta}\right]\bar{r}^{-\lambda_{ver}} +$$
$$\sigma^s_{r\theta}(\bar{r},\pi/2,\phi) = K^s_{1r\theta}L^*_{1r\theta}\left\{(\sin\phi)^{-\lambda_{side}}\cos\phi + (\cos\phi)^{-\lambda_{side}}\sin\phi\right\}\bar{r}^{-\lambda_{ver}} + \qquad (12)$$
$$\sigma^s_{\phi\theta}(\bar{r},\pi/2,\phi) = K^s_{1\phi\theta}L^*_{1\phi\theta}\left\{(\sin\phi)^{-\lambda_{sideA}}\cos\phi - (\cos\phi)^{-\lambda_{sideB}}\sin\phi\right\}\bar{r}^{-\lambda_{ver}} +$$

and the intensity of singularity at the vertex is defined as $K_{ij}^{3D} = K_{1ij}^{s} L_{1ij}^{*}$ in the present paper. The value of intensity includes the influence of the vertex and singularity lines on the stress singularity. The values of the intensity are listed in Table 5. It is found that the intensity of singularity in the stress component, $\sigma_{\theta\theta}$, relating to delamination of the interface is the largest value.

4. Conclusion

In the present paper, angular functions near the vertex on an interface in a three-dimensional bonded joint were derived from eigen analysis based on a finite element method. A relationship between angular functions for the vertex and for the stress singularity line was derived. The intensity of singularity at the vertex was defined considering the stress singularity in the radial direction from the vertex and that in the angle ϕ direction reflecting the influence of stress singularity line on the stress distributions. Finally, the values of the intensity of singularity were determined.

References

[1] T. Inoue, and H. Koguchi, Influence of the intermediate material on the order of stress singularity in three-phase bonded structure, Int J Solids Struct 33 (1996) 399-417

[2] H. Koguchi, T. Muramoto, The order of stress singularity near the vertex in three-dimensional joints, Int J Solids Struct 37 (2000) 4737-4762

[3] H. Koguchi, A. Taniguchi, Charcteristic of stress singularity field of residual thermal stresses at vertex in three-dimensional bonded joints, Trans Jp Soc Mech Eng 74 (742) (2008) 864-872

[4] D.B. Bogy, On the problem of edge-bonded elastic quarter-planes loaded at the boundary, Int J of Solids Struct 6 (1970) 1287-1313

[5] D.B. Bogy, Two edge-bonded elastic wedges of different materials and wedge angles under surface tractions, J Appl Mech 38 (1971) 377-386

[6] J.P. Dempsey, G.B. Sinclair, On the stress singularities in the plane elasticity of the composite wedge, J Elasticity 9 (1979) 373-391

[7] D. Leguillon, Computation of 3D singular elastic fields for the prediction of failure at corners, Key Engineering Materials 251-252 (2003) 147-152

[8] P.E.W. Labossiere, M.L. Dunn, Fracture initiation at three-dimensional bimaterial interface corners, J Mech Physi Solids 49 (2001) 609-634

[9] S.S. Pageau, Jr. S.B. Bigger, Finite element evaluation of free-edge singular stress fields in anisotropic materials, Int J Num Methods Eng 38 (1995) 2225-2239

[10] H. Koguchi, M. Yamaguchi, K. Nimaki, P. Monchai, Analysis of stress singularity fields in three-dimensional joints by three-dimensional boundary element method using fundamental solution for two-phase transversely isotropic materials, Trans Jp Soc Mech Eng 69 (2003) 585-593